

Velocity fluctuations in a homogeneous dilute dispersion of high-Reynolds-number rising bubbles

By FRÉDÉRIC RISSO† AND KJETIL ELLINGSEN‡

Institut de Mécanique des Fluides de Toulouse, UMR 5502 CNRS-INP-UPS, Allée C. Soula,
31400, Toulouse, France

(Received 26 March 2001 and in revised form 11 September 2001)

An experimental investigation of a homogeneous swarm of rising bubbles is presented. The experimental arrangement ensures that all the bubbles have the same equivalent radius, $a = 1.25$ mm. This particular size corresponds to high-Reynolds-number ellipsoidal rising bubbles. The gas volume fractions α is small, ranging from 0.5 to 1.05%. The results are compared with the reference situation of a single rising bubble, which was investigated in a previous work. From the use of conditional statistics, the existence of two regions in which the liquid velocity fluctuations are of a different nature are distinguished. In the vicinity of the bubbles, the liquid fluctuations are the same as those measured close to a single rising bubble. They therefore do not depend on α . Far from the bubble, the liquid fluctuations are controlled by the nonlinear interactions between the wakes of all the bubbles. Their probability density function scales as $\alpha^{0.4}$, exhibiting a self-similar behaviour. The total fluctuation combines the contributions of these two regions weighted by the fraction of the liquid volume they occupy. The contribution of the bubble vicinity is thus shown to vary linearly with α while the wake contribution does not. Both are non-isotropic since strong upward vertical fluctuations are more probable.

1. Introduction

Dispersed two-phase flows consist of a population of particles immersed in a fluid. They appear in many different situations including the sedimentation of drops in a liquid, the rise of bubbles in air-lift columns and turbulent pipe bubbly flows. However, whatever the nature of the case under consideration, low- or high-Reynolds-number regimes, laminar or turbulent situations, bubbles or drops, they have a common characteristic: the particle motions cause velocity fluctuations in the continuous phase. These stochastic fluctuations are of a different nature from those existing in single-phase flows. To emphasize the differences with the single-phase shear-induced turbulence, this phenomenon is sometimes called pseudo-turbulence.

This motivates investigations of flows in which the movement of the continuous phase is due only to the motions of the particles, especially the settling (resp. the rise) of heavy (resp. light) particles in a fluid otherwise at rest. The focus of the current work is on the liquid fluctuations induced by the rise of high-Reynolds-number bubbles.

† Author to whom correspondence should be addressed: e-mail. risso@imft.fr.

‡ Present address: Norsk Hydro ASA, Res. Centre Porsgrunn, PO box 2560, 3907, Norway.

However, since the knowledge of the sedimentation of small particles is more advanced, we first recall some important results originating from low-Reynolds-number studies.

In a pioneering work, Batchelor (1972) determined the average settling velocity V_s of a homogeneous dispersion of rigid spheres. He considered the problem in the Stokes regime and in the limit of small particle-volume-fractions α . The difficulty of this situation lies in the fact that the liquid velocity at a distance r from a single sphere of radius a falling at a velocity V varies asymptotically as Va/r . This slow decrease prevents us from obtaining a first approximation of the liquid velocity by summing the contributions of an indefinitely large number of particles because the corresponding integral diverges. The use of a renormalization method is thus necessary (see Hinch 1977 for a modern reformulation). The average settling velocity V_s is found to depend on the spatial distribution of the particles. Indeed, for a regular array of falling particles, the reduction in V_s varies as $\alpha^{1/3}$, although it varies as α when the particle locations are statistically independent. Using the same method, Caflisch & Luke (1985) calculated the velocity variance for a uniform distribution of the spheres. Surprisingly, they found that the variance increased unboundedly as the particle number increased. Later, Koch & Shaqfeh (1991) showed that a finite variance was obtained if the pair probability function of the sphere locations reflected a net deficit of one particle in the vicinity of each particle. To the best of our knowledge, the problem of sedimentation in the Stokes regime is not solved (see Brenner 1999; Lei, Ackerson & Tong 2001 and references therein for recent developments) and we point out the following result. When the velocity perturbation induced by the motion of a single particle decreases too slowly for its integral over the whole space to be convergent, the velocity fluctuations induced by a population of such particles can depend strongly on the spatial distribution of the particles, even in the low-volume-fraction limit.

Biesheuvel & van Wijngaarden (1984) addressed the problem of velocity fluctuations in a dilute dispersion of high-Reynolds-number spherical bubbles. They asserted that in this situation the wake was negligible compared to the potential flow and thus considered the problem in the potential flow limit. The potential velocity u induced by a single bubble decreases as $V(a/r)^3$. Contrary to the Stokes case, this decay is rapid enough to allow a straightforward calculation of the velocity variance from the summation of the contributions of individual bubbles. In a dilute dispersion, the liquid velocity correlations $\langle u_i u_j \rangle$ can thus be obtained by the integration of the velocity induced by a single bubble over the volume \mathcal{V} external to the bubble:

$$\langle u_i u_j \rangle = \frac{3\alpha}{4\pi a^3} \int_{\mathcal{V}} u_i u_j \, dv = \begin{pmatrix} 1/5 & 0 & 0 \\ 0 & 3/20 & 0 \\ 0 & 0 & 3/20 \end{pmatrix} \alpha V^2, \quad (1.1)$$

where direction 1 is along gravity and directions 2 and 3 are horizontal. The point is to determine whether this result is valid for real situations at finite Reynolds numbers. On the one hand, it is known that large-Reynolds-number bubbles may deform and undergo path oscillations. The potential calculation can be extended to deal with ellipsoidal bubble shapes and helicoidal trajectories (Lance & Bataille 1991). However, since the calculation is based on the linear summation of the individual bubble contributions, the variance of the fluctuations still varies linearly with α . On the other hand, numerous experimental investigations have shown that a wake develops behind rising bubbles (Maxworthy 1967; Bhagha & Weber 1981; Lunde & Perkins 1997; Brüker 1999; de Vries 2001). In a previous work (Ellingsen & Risso

2001 hereinafter referred to as I), we investigated the rise of a clean single air bubble of 1.25 mm radius in water. The velocity perturbation induced by the bubble passage was found to include two contributions, one due to the potential flow and the other due to the wake. Moreover, the wake contribution was significantly larger than that of the potential one.

Let us consider a bubble of axisymmetric shape rising rectilinearly. The liquid velocity in the far wake is quasi-parallel. It can be determined from a momentum balance over a large volume around the bubble (Batchelor 1967, p. 348):

$$\frac{u_z}{V} = \frac{1}{4\pi} \frac{D}{\rho v V z} \exp\left(-\frac{V}{4v} \frac{r^2}{z}\right), \quad (1.2)$$

where D is the total drag exerted on the bubble, r and z are the cylindrical radial and vertical coordinates, v and ρ are the liquid kinematic viscosity and density. We may expect to determine the contribution of the far wakes to the variance in a dilute dispersion of bubbles in the same way as for the derivation of (1.1):

$$\langle u_z^2 \rangle = \frac{3\alpha}{4\pi a^3} \int_{\theta=0}^{2\pi} \int_{z=z_0}^{\infty} \int_{r=0}^{\infty} u_z^2 r \, dr \, d\theta \, dz \quad (1.3)$$

As was already pointed out by Koch (1993), this integral diverges as $\ln z$ and it is not possible to determine the variance by summing the individual bubble contributions. The case investigated in I corresponded to an ellipsoidal bubble that undergoes path oscillations. The experimental results showed that the flow in the wake includes two contributions due to a quasi-steady wake that spreads around the bubble trajectory and wake vortices that are generated at the bubble rear. Nevertheless, these vortices do not significantly change the velocity decay in the far wake which remains similar to that existing behind a bubble rising rectilinearly; the problem of the divergence in (1.3) thus remains. It is only in the potential limit that the decrease of the velocity perturbations induced by a single bubble is fast enough. Bubbly flows at high, but finite, Reynolds numbers are thus as complicated as Stokes flows and are probably even more complicated since the interactions between the wakes are expected to be nonlinear.

Lance & Bataille (1991) carried out an experimental study of a homogeneous swarm of air bubbles rising in water. The radius of the bubbles was approximately 2.5 mm, which corresponded to a bubble Reynolds number, $Re = 2aV/v$, of approximately 1100. The authors measured the liquid velocity variance with a laser-Doppler anemometer (LDA). They found that the variance was proportional to the volume fraction for α ranging between 0.5% and 3% (see their figure 9). They concluded that the wake contribution represented less than 20% of the total variance—a level which was not detectable by their measuring technique, and that the total variance was controlled mainly by the potential contribution. Parthasarathy & Faeth (1990) and Mikuzami, Parthasarathy & Faeth (1992) investigated the pseudo-turbulence generated by a uniform flux of falling solid particles at very low volume fractions ($\alpha < 0.01\%$). By means of LDA, they determined the statistical properties of the fluctuations for particle Reynolds numbers ranging from 38 to 800. The results were compared with the prediction of a model based on the linear superposition of the potential and wake contributions generated by isolated particles. They overcome the difficulty of the non-convergence of the integral (1.3) by stopping the integration at a given distance z_0 behind the bubble. This distance was fixed in order to match the experimental results ($z_0 \sim 350a$). This was justified by assuming that only the

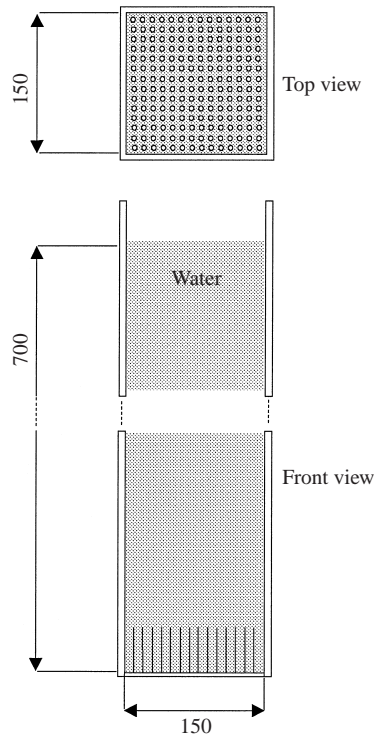


FIGURE 1. The test section (not to scale, lengths in mm).

near-field region of the wake would maintain sufficient coherence to contribute to flow properties as a wake. Under this assumption, the model prediction was in fairly good agreement with the measurements. The authors nevertheless concluded that a more reasonable solution for the convergence problem has to be found.

The current study is an experimental investigation of an homogeneous dispersion of high-Reynolds-number rising bubbles. The goal is to clarify the nature of the velocity fluctuations induced by the bubble motions for moderate gas volume fractions. This implies that it is necessary to make a clear distinction between the role of the flow induced by each bubble (potential flow, near and far wakes) and the effect of hydrodynamic interactions between the wakes. Our strategy consists of comparing the velocity statistics in the swarm of bubbles with the reference situation of a single rising bubble. The differences observed between these two situations will characterize the hydrodynamic interactions. In I, we have investigated in detail the rise of a single bubble ($a = 1.25$ mm, $Re = 800$). Since this instance corresponds to an ellipsoidal bubble behind which a very long wake develops, it is particularly well suited for the analysis of wake interactions. Here, we thus chose to study a spatially homogeneous swarm of bubbles of this particular size. The use of a single bubble size and the absence of volume-fraction gradients will allow us to focus on the specific role of the volume fraction.

2. Experimental facility and instrumentation

The test section is shown in figure 1. It is an open tank of 700 mm height with a square cross-section of 150 mm width. To allow full optical access, the four sides

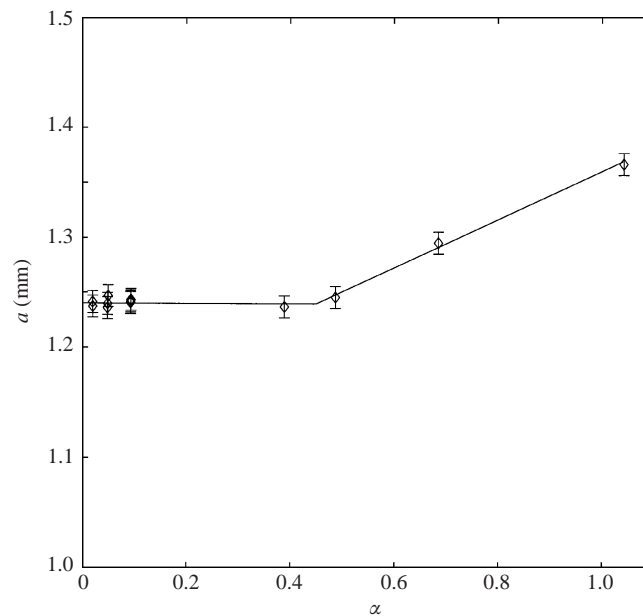


FIGURE 2. Bubble equivalent radius against the gas volume fraction.

are of glass construction. The tank is filled with tap water and the air is injected at the bottom by a regular array of 14×14 stainless-steel capillary tubes (150 mm long, inside/outside diameter 0.33/0.50 mm). Since all the tubes are connected to the same pressure-controlled air tank, they all supply the same flow rate. Note that the experimental facility is the same as the one used in I to investigate the case of a single rising bubble. It was established that the tank was wide enough not to limit the development of the long wake that takes place behind isolated bubbles. Moreover, it was checked that the flow dynamics was not influenced by the presence of surface-active contaminants. In the current experiments, the gas volume fraction α is varied between 0.5% and 1.05% by adjusting the total air-flow rate. In this injection regime, the bubbles detach periodically from the tip of each capillary. The bubble size has been measured just above the injection from high-speed video imaging by using the same procedure as in I. The result is shown in figure 2. For α less than 0.5%, the bubble shape is an oblate ellipsoid with an equivalent radius of 1.24 ± 0.01 mm and an aspect ratio of 2.05. When α is increased from 0.5% to 1.05%, the equivalent radius increases slightly up to 1.37 mm. For the range of elevations investigated, the effect of the reduction in hydraulic pressure on the bubble diameter is less than 1%. For the gas volume fractions and bubble residence times considered, coalescence was not observed. The maximal variation of the bubble diameter is thus approximately 10% and leads to a variation of the bubble rise velocity of less than 1%. The effect of the bubble size variation is consequently negligible compared to that of α and will hereinafter be neglected.

A double optical-fibre probe is used to detect the presence of air at two points separated by a vertical distance $h = 3.1$ mm. The probes have a diameter of $50 \mu\text{m}$ and pointed ends. Each probe provides an electric signal, the magnitude of which is drastically different depending on the phase surrounding the probe tip. This analogue signal is converted into a digital signal and recorded by a computer. A threshold is then applied to obtain the characteristic function of the gas phase. To complete

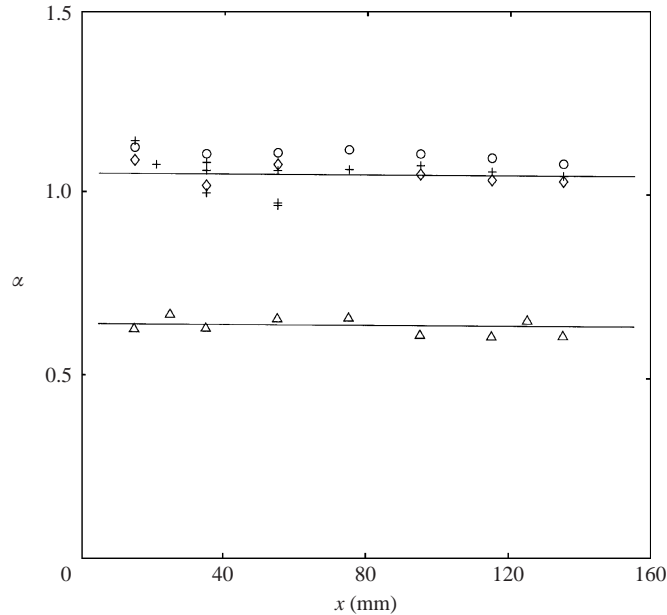


FIGURE 3. Horizontal profiles of the local gas volume fraction: \triangle , first air flow rate $\langle \alpha \rangle = 0.64\%$ at $z = 300$ mm; $+$, second air flow rate $\langle \alpha \rangle = 1.05\%$ at $z = 100$; \diamond , 300; \circ , 500 mm.

this treatment, two parameters have to be adjusted: the threshold and the sampling frequency. The threshold value was determined from the comparison between the probe signal and a simultaneous detection of the bubble interface by high-speed imaging. With a sample frequency of 10 kHz, this procedure allows us to obtain the interface arrival time with an accuracy of 0.1 ms. Concerning the gas volume fraction, it is also important to use a recording duration, T_{total} , large enough to ensure the statistical convergence. Here, T_{total} was fixed to 30 mn. This led to an accuracy of 3% in the value of α . Figure 3 shows different horizontal profiles of the local gas volume fraction. The results correspond to two air-flow rates and three elevations. For the smallest average volume fraction, $\langle \alpha \rangle = 0.64\%$, the local volume fraction is constant within the measurement accuracy ($\pm 3\%$); for the largest one, $\langle \alpha \rangle = 1.05\%$, the scatter is slightly larger ($\pm 8\%$). The bubble swarm can consequently be considered to be statistically uniform. We also checked this uniformity by measuring the velocity statistics at different points in the tank; the results never depended on the location. In the following, all the measurements had been collected at a single point located at the tank centreline and 300 mm above the tips of the capillaries.

The liquid velocity is measured by a laser-Doppler anemometer (LDA). The LDA system is the same as in I. It provides measurements of the vertical component of the liquid velocity (z -direction) and of one horizontal component (x -direction). The two measuring volumes are ellipsoids with a major axis of 0.15 mm in the y -direction and 0.04 mm in the x - and z -directions. In I, this system was used in combination with three-dimensional bubble-interface detection by high-speed imaging and was proved to measure accurately the liquid velocity around a single rising bubble, provided the distance to the interface was at least 0.1 mm. Here, the presence of many bubbles around the measuring volume causes two major problems. First of all, spurious measurements are detected when a bubble intersects the laser beams close to the measuring volume. The number of these spurious samples is of order α and depends on

the adjustment of the LDA parameters (laser-source power, photomultiplier voltage and electric amplifier gain). These spurious samples correspond to large velocity fluctuations ranging from 0.7 to 1.2 times the bubble velocity V . The probability density function (p.d.f.) of the liquid velocity is consequently not affected in the range from $-0.7V$ to $0.7V$. Concerning the variance, the presence of these spurious measurements add a wrong contribution ($\propto \alpha V^2$) that can be of the same order of magnitude as the actual variance. To obtain a variance that did not depend on the LDA system adjustment, Marié (1983) proposed to reject the velocity samples that were larger than a given threshold. This technique, also used by Lance & Bataille (1991), leads to reproducible results. In the vicinity of the bubbles there are, however, also correct velocity samples between $0.7V$ and $1.2V$. Consequently, since this technique excluded the large velocity fluctuations detected close to the bubbles, it underestimates the liquid velocity variance. From our experience, there is no accurate and reliable technique to obtain the liquid velocity variance in the presence of high-Reynolds-number highly deformed bubbles in situations where the mean liquid velocity is zero. (See Ellingsen *et al.* 1997; Suzanne *et al.* 1998 for a detailed discussion.) After many attempts, we did not manage to solve this problem satisfactorily. Consequently, we will not present here results concerning the velocity variance. Our strategy will be based on two points: (i) comparing the p.d.f. of the velocity fluctuations measured in the vicinity of the bubbles with that obtained close to a single rising bubble and (ii) determining the properties of the total p.d.f. in the range $-0.7V$ – $0.7V$. The second problem that was related to the presence of many bubbles was also pointed out by Marié (1983). It is the existence of spurious zero-velocity measurements. In the absence of the optical probe, we managed to suppress these erroneous data by a suitable adjustment of the LDA optical and electronic arrangements (Ellingsen 1998).

In order to investigate the velocity field around the bubbles, the LDA and the optical probe were used simultaneously. The centre of the LDA measuring volume was located 0.6 mm below the tip of the optical probe. This separation was just a little smaller than the minor axis of the bubbles (0.77 mm). The detection of an interface by the optical probe thus coincided with the passage of a bubble through the measuring volume. The bubble arrival times were stored by the LDA processor in the same file as the LDA velocity samples. This allowed the determination of the time interval between each velocity sample and the closest detected bubble. In §4.1, we will use this information to analyse how the velocity fluctuations depend on the distance to the bubbles. Owing to the small size of the optical probe, its presence above the LDA measuring volume had no significant influence on the flow. It nevertheless caused the reappearance of a few zero-velocity erroneous measurements. These only have an influence on the zero-velocity class of the p.d.f. of the velocity fluctuations.

3. Bubble positions and velocities

The objective of this section is to determine how the bubble positions and velocities are modified by the presence of the other bubbles. Before we analyse the bubble swarm, let us recall the results obtained in I concerning the reference situations of a single rising bubble. After an initial acceleration stage, the bubble undergoes path oscillations. During these oscillations the bubble takes a constant shape similar to an oblate ellipsoid of aspect ratio 2.05. The bubble-centre velocity is at each instant parallel to the bubble symmetry axis and its magnitude, V , remains almost constant (325 mm s^{-1}). The time evolution of the bubble-centre coordinates in a frame where

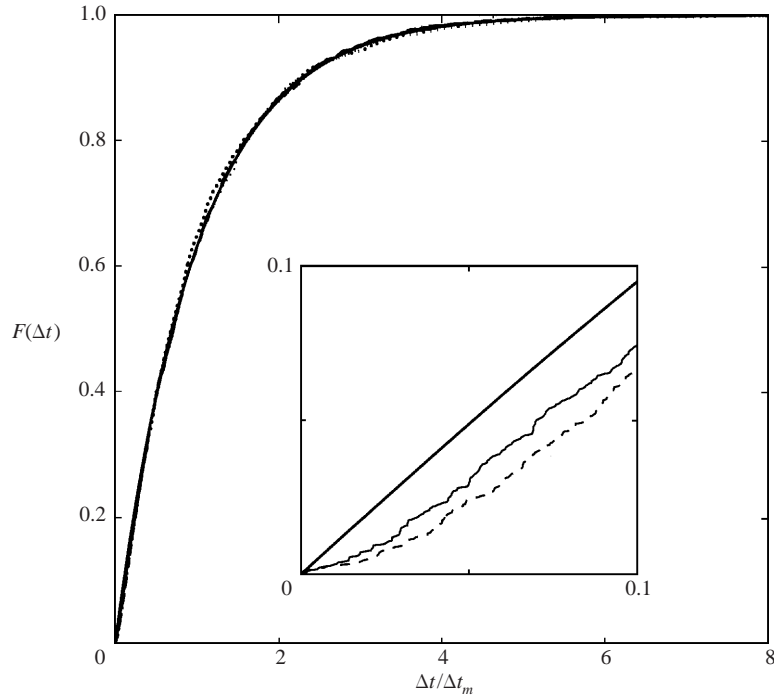


FIGURE 4. Distribution functions of the time intervals between consecutive bubbles: —, Poisson's process (equation (3.2)); \cdots , $\alpha = 0.52\%$ ($\Delta t_m = 0.70$ s); —, 0.64% ($\Delta t_m = 0.64$ s); $\cdot\cdot\cdot$, 0.78% ($\Delta t_m = 0.51$ s); $-\cdot-$, 0.92% ($\Delta t_m = 0.48$ s); $---$, 1.05% ($\Delta t_m = 0.44$ s). The windowed graph is an enlargement of the figure for short time intervals (for clarity, only three curves are presented).

the x -direction coincides with the principal direction of oscillations are given by:

$$\left. \begin{aligned} x_b &= L_x \sin(\omega t), \\ y_b &= \pm L_y \cos(\omega t), \\ z_b &= L_z \sin(2\omega t + \pi) + V_z t, \end{aligned} \right\} \quad (3.1)$$

where $\omega = 39 \text{ rad s}^{-1}$, $L_x = 4.3 \text{ mm}$, $L_z = 0.35 \text{ mm}$, $V_z = 300 \text{ mm s}^{-1}$ and L_y is small compared to L_x and takes random values.

We saw in the introduction that the spatial distribution of the bubbles can have a major influence on the velocity statistics. Here, the gas volume fraction was found to be uniform all over the test section. However, this does not ensure that the position of one bubble is statistically independent from the others. It is possible to obtain information about the pair probability of the bubble positions from the data provided by the optical probe. If the bubbles were points with independent positions, the statistics of the time intervals between the arrival at the first probe of two consecutive bubbles should constitute a Poisson's process. The distribution function $F(\Delta t)$ of such a process, which is the probability that the time separation δt between two consecutive events is larger than Δt , is given by:

$$F(\Delta t) = \text{Prob}(\delta t < \Delta t) = 1 - \exp(-\Delta t/\Delta t_m), \quad (3.2)$$

where Δt_m is the average time separation. Since the bubbles cannot penetrate each other, any experimental distribution necessarily differs from Poisson's law. For spherical bubbles, we might expect the pair probability to be equal to zero for separations

smaller than the bubble diameter and constant for larger separations. This pair probability distribution is, however, not a solution of the associated Liouville's equation. The fact that the bubbles cannot overlap is therefore responsible for an ordering of the bubble positions on a distance that is larger than the bubble diameter. Figure 4 shows the experimental distribution functions $F(\Delta t/\Delta t_m)$ for five different gas volume fractions. Here, the analysis of the results is complicated by the fact that the bubbles are oblate ellipsoids and that the present measurement technique only provides information concerning the bubble separations in the vertical direction. For short separations, the experimental distributions show a deficit of bubble occurrences compared to Poisson's law. An estimate of the range of the repelling force that acts between the bubbles is given by the time separation Δt_r at which the experimental distributions reach the slope of Poisson's law. It is found that Δt_r is approximately equal to 15–20 ms, which corresponds to a vertical separation $\Delta z_r = \Delta t_r V_z = 3.5\text{--}5a$. For larger separations, all the experimental distributions are close to Poisson's law. However, this does not exclude the possibility of a weak long-range ordering of the bubble positions. Let us remember that, in low-Reynolds-number situations, Koch & Shaqfeh (1991) showed that a net deficit of one bubble in the region surrounding each bubble was sufficient to cause the screening of the velocity fluctuations. Only a very accurate counting of the number of bubbles within regions of given volume (not possible here owing to the width of the container) can detect such a minute variation (see Lei *et al.* 2001). The present results nevertheless clearly indicate that there are no large-scale clusterings. In particular, the horizontal rafts of bubbles predicted by Sangani & Didwania (1993) from potential calculations and observed in experiments by Zenit, Koch & Sangani (2001) for spherical high-Reynolds-number bubbles do not take place here.

The focus is now on the bubble velocities. When a bubble rises up through the double optical probe its front part is successively detected by each of the two probes. The probe separation h divided by the time interval $\delta\tau$ between these two events is a measure of the interface velocity. However, since the bubbles are not spherical and undergo path oscillations, $h/\delta\tau$ is not the vertical component of the bubble velocity but combines the three-dimensional bubble displacements (translations and rotations). To obtain the reference situation corresponding to vanishing volume fractions, we calculated the p.d.f. of $h/\delta\tau$ corresponding to a succession of non-interacting bubbles. A virtual bubble was released from random positions and phases and its displacements calculated using (3.1). (The occurrences of L_y were given by the experimental statistics obtained in I for a single rising bubble at the same distance from the injection.) The intersections of the interface with two points separated by a distance h were then calculated. This was repeated for a large numbers of bubbles and the reference p.d.f. for non-interacting bubbles was thus obtained. The result is represented by the thick plain line in figure 5. From (3.1), the vertical velocity of a single bubble is constant with an average $V_z = 300\text{ mm s}^{-1}$ and standard deviation of $0.064V_z$. However, the average value of $h/\delta\tau$ is larger than the mean rise velocity ($1.21V_z$) and its standard deviation is significant ($0.16V_z$). Figure 5 also shows the experimental p.d.f. corresponding to three different gas volume fractions ($\alpha = 0.52, 0.78, 1.05\%$). For $\alpha = 0.52\%$, the statistics of $h/\delta\tau$ are the same as those of isolated bubbles (the average value differs by less than 3% and the standard deviation by less than 0.4%). For larger α , the standard deviation slightly increases to reach $0.18V_z$ at $\alpha = 1.05\%$. It can thus be concluded that the fluctuations of the bubble motions are driven by the same mechanism of path oscillations as for a single bubble. Hydrodynamic interactions between bubbles do not influence the bubble motion for α less than 0.5%

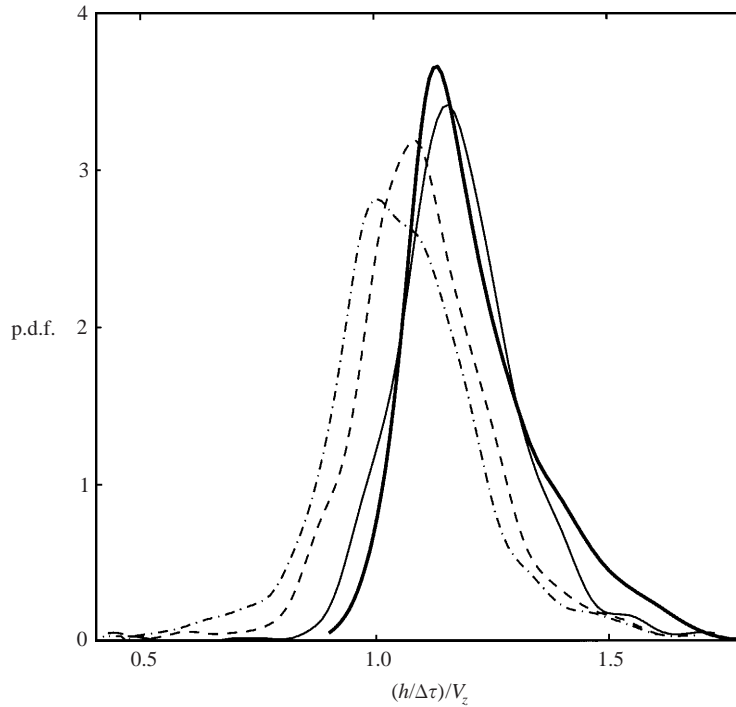


FIGURE 5. Probability density function of the interface velocities: —, $\alpha = 0$ (single rising bubble); — —, 0.52%; — · —, 0.78%; · · ·, 1.05%.

and only cause a small increase of the intensity of the fluctuations in the range of α investigated.

4. Liquid velocity fluctuations

In the previous section we showed that the hydrodynamic interactions play a minor role in the bubble behaviour, which remains almost the same as for isolated bubbles. The point is now to determine how the interactions modify the liquid velocity. Our analysis will involve two parts. First, we will compare the velocity field induced by a single rising bubble with the one measured in the vicinity of the bubbles that belong to the homogeneous swarm. Secondly, we will investigate the liquid velocity fluctuations without considering the bubble locations. From the differences between the statistics of the liquid velocity conditioned or not by the presence of the bubbles, we intend to distinguish between the signature of individual bubbles and hydrodynamic interactions.

4.1. Velocity statistics conditioned by the bubble presence

The present analysis is based on the simultaneous measurements of the liquid velocity and bubble arrival times. We know the time interval t_b between each velocity sample and the passage of a bubble through the measuring point. It is therefore possible to arrange the velocity samples in increasing order of t_b . The time interval t_b can then be converted into the spatial vertical separation, $Z = V_z t_b$. The evolution of the liquid velocity against the vertical distance from a bubble is thus obtained. This treatment was applied to the measurements of five volume fractions ($\alpha = 0.52, 0.64, 0.78, 0.92$

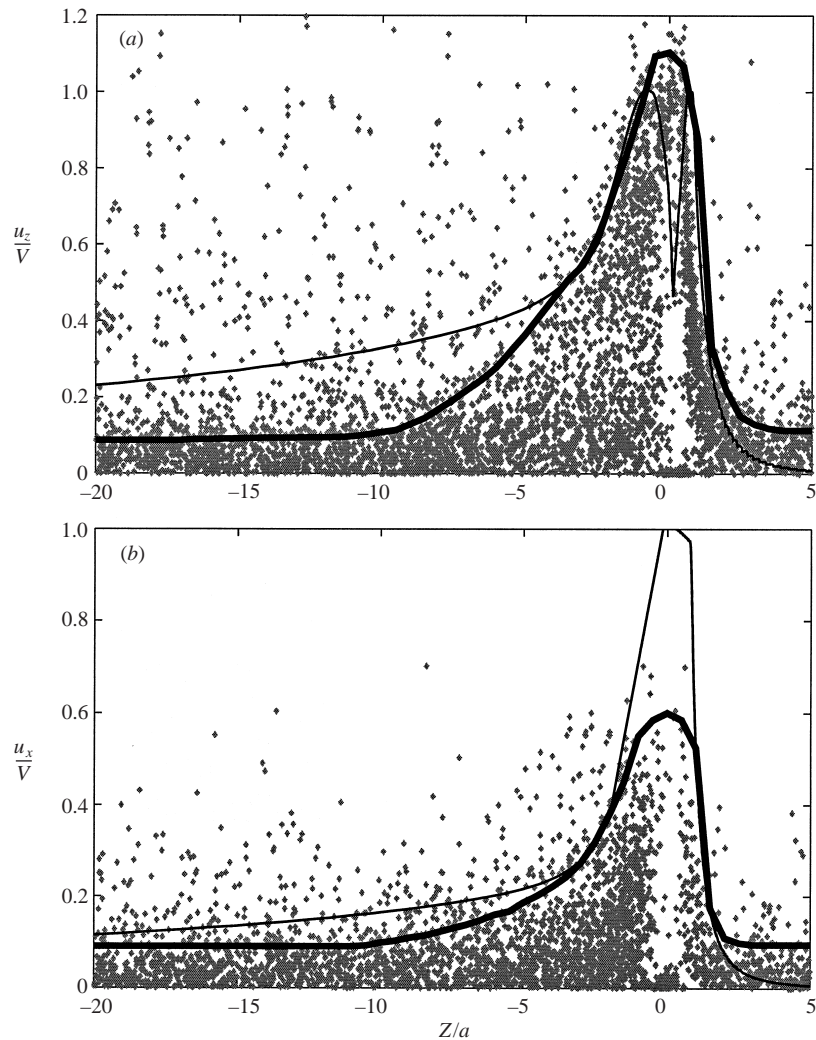


FIGURE 6. Liquid velocity against the distance to the closest bubble: (a) vertical and (b) horizontal components; \blacklozenge , measured velocity samples; —, contour line; —, maximal velocity close to a single rising bubble (from I).

and 1.05%); depending on the experimental set under consideration, the number of detected bubbles ranged from 2250 to 3350. Here, we only present the case $\alpha = 0.52\%$ since the results were found to be independent of α . Figures 6(a) and 6(b) show, respectively, the vertical (u_z) and horizontal (u_x) components of the liquid velocity. Each symbol represents a velocity sample measured before ($Z > 0$) or after ($Z < 0$) a bubble passage. The density of symbols near each pair (Z, u_i) is a measure of the probability of the corresponding event. Since a bubble that does not touch the optical probe can be closer to the measuring volume than any detected bubble, the maximum measured velocity is the same for all Z . However, in a homogeneous dispersion, the probability that two different bubbles are close to the same point is α times smaller than the probability that only one bubble is present (see Hinch 1977). Consequently, for most of the samples, Z is actually the vertical distance to the closest bubble. The frontier between these true samples and the wrong ones is delimited by the sharp

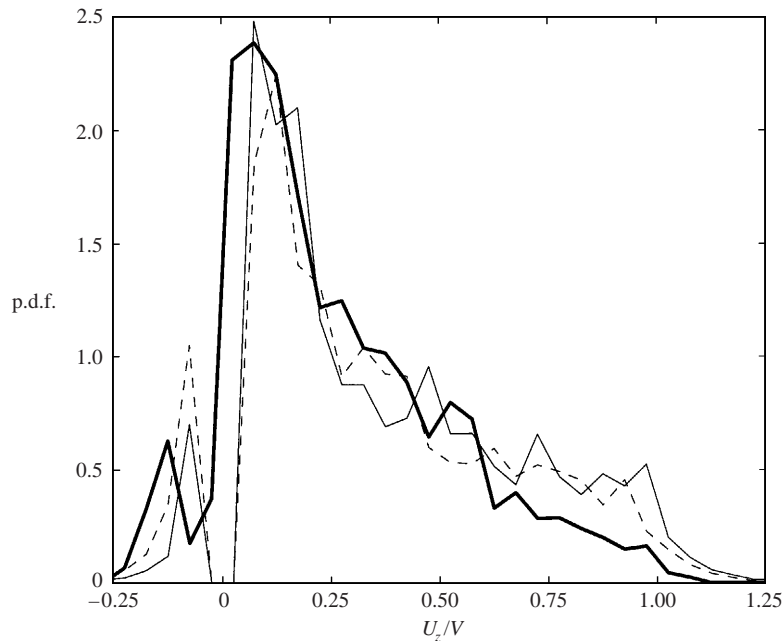


FIGURE 7. Probability density function of the liquid vertical fluctuations in the vicinity of the bubbles: —, $\alpha = 0$ (single rising bubble); — — —, 0.64%; - - -, 1.05%.

variation in the density of symbols that is clearly visible for each Z . This contour line is indicated by the thick line in figure 6. It corresponds to the maximum velocity over all the possible bubble orientations and horizontal positions that exist at a given vertical distance Z from a bubble. Figure 6 also shows the maximal velocity that exists close to a single rising bubble. The comparison between the results obtained inside the bubble swarm and close to the single rising bubble indicates the existence of three regions. In the vicinity of the bubble ($-5 < Z/a < 5$), the flow is similar to that induced by a single rising bubble: potential in front of the bubble and controlled by the wake behind. Further behind the bubble ($-10 < Z/a < -5$), the interactions become significant and the liquid velocity decreases much faster than behind a single bubble. For larger distances ($Z < -10a$), the velocity fluctuations finally reach an asymptotic state that is independent of the distance from the bubble.

These results suggest that we should carry out a specific study of the velocity statistics in the vicinity of the bubbles. The p.d.f. of the liquid-velocity fluctuations was calculated by retaining only the velocity samples detected at a distance $|Z|$ less than $5a$ from any bubble. Note that the sample class corresponding to velocities ranging between $-0.01V$ and $0.01V$ contains spurious zero-velocity samples (see §2). This has no significant influence on the p.d.f. of the vertical velocity; the corrupted class, which contains only a few samples, will simply be discarded. In contrast, the p.d.f. of the horizontal velocity is strongly altered since the most probable horizontal velocity is zero. Consequently, only the p.d.f. of the vertical velocity is presented here. The results are plotted in figure 7 for two different volume fractions ($\alpha = 0.64$ and 1.05%). First of all, it is clear that the statistics of the fluctuations do not depend on α . (This result was confirmed by the matching of all the other measured p.d.f. in the range of α investigated.) Furthermore, there are no significant differences with the p.d.f. corresponding to a single rising bubble, rather there are only more velocity

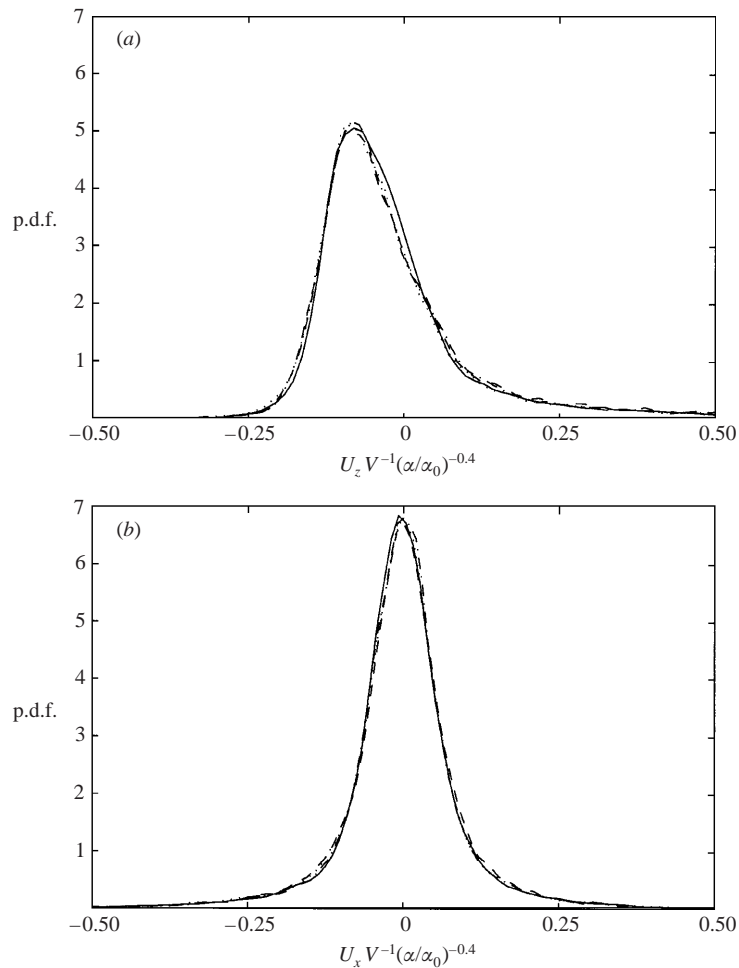


FIGURE 8. Probability density function of the total liquid fluctuations normalized by $(\alpha/\alpha_0)^{0.4}$ with $\alpha_0 = 0.64\%$: (a) vertical component; (b) horizontal component; —, $\alpha = 0.64\%$; ···, 0.78% ; - · - ·, 0.92% ; - - -, 1.05% .

samples than for an isolated bubble between 0.7 and $1.25V$. This result is, however, not surprising since this velocity range contains spurious samples and also a few data measured close to a non-detected bubble.

Finally, the following conclusions are obtained for gas volume fractions ranging between 0.5 and 1.05% . In the vicinity of each bubble ($-5 < Z/a < 5$), the velocity fluctuations are controlled by the flow induced by this particular bubble and are therefore independent of the volume fraction. On the other hand, although the wake behind a single rising bubble is very long (velocities as large as $0.05V$ were detected up to $Z = -150a$), the hydrodynamic interactions have totally destroyed the individual wakes at only $10a$ behind the bubbles.

Koch (1993) proposed a theory for the velocity fluctuations in a sedimenting suspension where particles have Oseen's wakes. He considered the possibility that the wake behind a particle in a suspension spreads and therefore decays faster than behind an isolated particle owing to the Reynolds stress associated with the motion of the other particles. In the range of Reynolds numbers that he considered ($1 \lesssim Re \lesssim 10$),

this effect was small and the intensity of the velocity fluctuations was controlled by a screening mechanism due to a deficit of particles in the wakes of a test particle. In contrast, for the large Reynolds number considered here, the very rapid decay of the wake indicates that the major effect is probably the enhancement of the wake spreading by the fluctuations generated by the other particles. Anticipating the results of the next section, a crude estimate of the velocity magnitude characteristic of the spreading mechanism is given by the width (defined by retaining 95% of the samples) of the p.d.f. of the unconditioned horizontal velocity fluctuations (figure 8):

$$u_{spread} \approx 0.44 V (\alpha/\alpha_0)^{0.4}. \quad (4.1)$$

We thus find that u_{spread} increases from $0.40V$ at $\alpha = 0.52\%$ to $0.53V$ at $\alpha = 1.05\%$. Moreover, it seems reasonable that the distance l_z from which the decay of the wake becomes faster corresponds to the location where the vertical velocity behind a single bubble becomes equal to u_{spread} . From figure 6 we thus obtain an estimate of l_z close to $5a$, which is in good agreement with the velocity decay measured in the bubble swarm. In addition, the weak dependence of u_{spread} with the volume fraction could explain why no significant variation of l_z is detected in the range of α investigated.

4.2. Unconditioned velocity statistics

We now consider all the velocity samples without taking into account the bubble positions. Since the optical probe was no longer needed, it was removed from the test section. As a consequence, the measurements presented in this section are without erroneous samples and statistical bias in the range from $-0.5V$ to $0.5V$. Figure 8 shows the p.d.f. of the vertical and horizontal velocity fluctuations for four different volume fractions ($\alpha = 0.64, 0.78, 0.92$ and 1.05%). Since the hydrodynamic interactions have been shown to cause a strong attenuation of the wake that follows each bubble, we would expect that the velocity fluctuations scale as α^n with an exponent n between 0 and 1. In order to check this idea, the liquid velocity has been normalized by α^n . The value of n that provided the best scaling was indeed found to be $n = 0.4 \pm 0.02$. As shown in figure 8, this normalization leads to an excellent matching of all the p.d.f. over their whole range of variation, indicating that their behaviour is self-similar when α is varied. Although the vertical and horizontal fluctuations have the same dependence on α , their statistics are different. While the p.d.f. of the horizontal fluctuations is symmetric, the p.d.f. of the vertical fluctuations is strongly asymmetric, intense fluctuations occurring more frequently in the upward direction than in the downward direction. This shows that, even if the liquid flow field is homogeneous, it is not isotropic.

5. Discussion

The present study provides original experimental results concerning a homogenous swarm of rising bubbles for gas volume fractions ranging between 0.5 and 1.05%. The bubbles all have approximately the same size ($a = 1.25$ mm), which corresponds to a Reynolds number, based on the bubble velocity, of 800 and a bubble aspect ratio of 2. Their behaviour is found to be weakly influenced by the hydrodynamic interactions: there are no bubble clusters, the bubble rise velocity is similar to that of a single rising bubble and the velocity fluctuations are mainly due to the periodic path oscillations of individual bubbles.

Concerning the liquid velocity, two regions have to be distinguished. In the vicinity

of each bubble, the flow is similar to that generated by a single rising bubble: potential in front of and alongside the bubble, and controlled by the wake behind. As a consequence, the statistics of the fluctuations herein do not depend on α (figure 7). In the range of volume fractions investigated, the vertical length l_z of this region is close to 5 bubble radii and depends very slightly on α . The fraction of the total volume this region occupies is thus proportional to $\alpha(l_z/a)^3$. On the other hand, the volume of the complementary region located far from the bubbles is proportional to $1 - \alpha(l_z/a)^3$. The velocity fluctuations are therein controlled by the nonlinear interactions between the wakes of all the bubbles and evolves in a self-similar manner as $\alpha^{0.4}$.

The p.d.f. of the total fluctuations is the sum of the p.d.f. of these two regions weighted by the respective fraction of the total volume they occupy (for small α it is not relevant to distinguish the liquid volume from the total volume). The vicinity of the bubble thus generates a contribution which is proportional to α while the region far from the bubble produces a nonlinear contribution. For small α , the vicinity of the bubbles contributes to a small part of the total amount of velocity samples. Since these samples represent most of the fluctuations in the range from $0.7V$ to $1.2V$, the contribution of the bubble vicinity to the total p.d.f. consists mainly of a small bump at large velocity fluctuations. In the range of α investigated here, the linear contribution has indeed no significant influence on the p.d.f. in the interval from $-0.5V$ to $0.5V$. The p.d.f. plotted in figure 8 thus represents the signature of the sole wake interactions. Nevertheless, since the variance is more sensitive to large fluctuations, its value can be strongly affected by the few events detected in the vicinity of the bubble. The present results are thus not in contradiction with those of Lance & Bataille (1991) who exhibited a linear dependence of the variance on α . For α between 0 and 1% the scatter in their results did not allow them to draw any conclusion while for α between 1 and 3%, the linear contribution to the variance seemed to dominate the nonlinear contribution, which was consequently not detectable with the instrumentation they used.

It is worth noting that the linear contribution to the velocity fluctuations does not involve the sole potential flow around the bubble. Figure 6 indeed shows clearly the importance of the near-wake in the region just behind the bubble. For very low volume fractions, Parthasarathy & Faeth (1990) and Mikuzami *et al.* (1992) also showed that the wake has to be taken into account in the linear contribution. For the extremely small α they considered ($\alpha < 0.01\%$), the size of the region around each particle that was not influenced by the hydrodynamic interactions was much larger than in the present work. This explains why they needed to consider individual wakes up to $350a$ behind each particle and why the linear summation of individual particle contributions matched the results approximately. Unfortunately, their approach required the length of the wake to be arbitrarily fixed to avoid the divergence of their calculation because the wake destruction is caused by the nonlinear interactions.

To conclude, the present results show that there are two regions in which the properties of the liquid velocity fluctuations are different. The statistics of the velocity fluctuations in each of these two regions were fully characterized for a particular bubble size which corresponded to a Reynolds number $Re = 800$. This regime is especially interesting since the hydrodynamic interactions destroy the long individual wakes that exist behind single rising bubbles and produce fluctuations that depend nonlinearly on the gas volume fraction. As far as we know, the current results constitute the first experimental characterization of the nonlinear interactions that take place at high Reynolds numbers. A deeper understanding of the bubble-induced liquid-velocity fluctuations now requires a theoretical model for these interactions.

REFERENCES

- BATCHELOR, G. K. 1967 *An Introduction to Fluid Dynamics*. Cambridge University Press.
- BATCHELOR, G. K. 1972 Sedimentation in dilute dispersions of spheres. *J. Fluid Mech.* **52**, 245–268.
- BHAGHA D. & WEBER M. E. 1981 Bubbles in viscous liquids: shapes, wakes and velocity. *J. Fluid Mech.* **105**, 61–85.
- BIESHEUVEL, A. & VAN WIJNGAARDEN, L. 1984 Two-phase flow equations for a dilute dispersion of gas bubbles in liquid. *J. Fluid Mech.* **148**, 301–318.
- BRENNER, M. P. 1999 Screening mechanisms in sedimentation. *Phys. Fluids* **11**, 754–772.
- BRÜCKER C. 1999 Structure and dynamics of the wake of bubbles and its relevance for bubble interaction. *Phys. Fluids* **11**, 1781–1796.
- CAFLISCH, R. E. & LUKE, H. C. 1985 Variance in the sedimentation speed of a suspension. *Phys. Fluids* **28**, 759–760.
- ELLINGSEN, K. 1998 Hydrodynamique des écoulements pilotés par l'ascension de bulles d'air virevoltantes. Thèse de doctorat, I.N.P. Toulouse, #1474.
- ELLINGSEN, K. & RISSO, F. 2001 On the rise of an ellipsoidal bubble in water: oscillatory paths and liquid induced velocity. *J. Fluid Mech.* **440**, 235–268.
- ELLINGSEN, K., RISSO, F., ROIG, V. & SUZANNE, C. 1997 Improvements of velocity measurements in bubbly flows by comparison of simultaneous hot-film and laser-Doppler anemometry signals. *Proc. ASME Fluid Engng Div. Summer Meeting, Vancouver, Canada, paper 97-3529*.
- HINCH, E. J. 1977 An average-equation approach to particle interactions in a fluid suspension. *J. Fluid Mech.* **83**, 695–720.
- KOCH, D. L. 1993 Hydrodynamic diffusion in dilute sedimenting suspensions at moderate Reynolds numbers. *Phys. Fluids* **A5**, 1141–1155.
- KOCH, D. L. & SHAQFEH, E. S. G. 1991 Screening in sedimenting suspensions. *J. Fluid Mech.* **222**, 275–303.
- LANCE, M. & BATAILLE, J. 1991 Turbulence in the liquid phase of a uniform bubbly air–water flow. *J. Fluid Mech.* **222**, 95–118.
- LEI, X., ACKERSON, B. J. & TONG, P. 2001 Settling statistics of hard sphere particles. *Phys. Rev. Lett.* **86**, 3300–3303.
- LUNDE K. & PERKINS R. J. 1997 Observations on the wake behind spheroidal bubbles and particles. *Proc. ASME Fluid Engng Div. Summer Meeting, Vancouver, Canada, paper 97-3530*.
- MARIÉ, J. L. 1983 Investigation of two-phase bubbly flows using laser anemometry. *PCH Physico-Chem. Hydro.* **4**, 89–95.
- MAXWORTHY, T. 1967 A note on the existence of wakes behind larges rising bubbles. *J. Fluid Mech.* **270**, 367–368.
- MIKUZAMI, M., PARTHASARATHY, R. N. & FAETH, G. M. 1992 Particle-generated turbulence in homogeneous dilute dispersed flows. *Intl J. Multiphase Flow* **18**, 397–412.
- PARTHASARATHY, R. N. & FAETH, G. M. 1990 Turbulence modulation in homogeneous dilute particle-laden flows. *J. Fluid Mech.* **220**, 485–514.
- SANGANI, A. S. & DIDWANIA, A. K. 1993 Dynamic simulations of flows of bubbly liquids at large Reynolds numbers. *J. Fluid Mech.* **250**, 307–337.
- SUZANNE, C., ELLINGSEN, K., RISSO, F. & ROIG, V. 1998 Local measurements in turbulent bubbly flows. *Nucl. Engng Des.* **184**, 319–327.
- DE VRIES, A. W. G. 2001 Path and wake of a rising bubble. PhD dissertation. University of Twente.
- ZENIT, R., KOCH, D. L. & SANGANI, A. S. 2001 Measurements of the average properties of a suspension of bubbles rising in a vertical channel. *J. Fluid Mech.* **429**, 307–342.